Materials Transactions, Vol. 43, No. 8 (2002) pp. 1858 to 1863
Special Issue on Lead-Free Electronics Packaging

Effect of Isothermal Aging on Ball Shear Strength in BGA Joints with Sn–3.5Ag–0.75Cu Solder

Chang-Bae Lee[1], Seung-Boo Jung[1, *], Young-Eui Shin[2] and Chang-Chae Shur[1]

[1]*Department of Advanced Materials Engineering, Sungkyunkwan University, 300 Chunchun-dong, Jangan-gu, Suwon 440-746, Korea*
[2]*Deparment of Mechanical Engineering, Chungang University, 221 Heuksuk-dong, Dongjak-ku, Seoul 150-756, Korea*

The ball shear strength of BGA solder joints during isothermal aging was studied with Sn–3.5Ag–0.75Cu solder on three different pads (Cu, electroless Ni–P/Cu, immersion Au/Ni–P/Cu) at temperature between 70 and 170°C for times ranging from 1 to 100 days. The reliability of solder ball attachment was characterized by mechanical ball shear tests. As a whole, the shear strength of BGA joints decreased with increasing temperature and time. The shear strength for both the immersion Au/Ni–P/Cu and electroless Ni–P/Cu pads was consistently higher than that of the Cu pad for all isothermal aging conditions. The fracture surface showed various characteristics depending on aging temperature, time, and the types of BGA pad. The P-rich Ni layer formed at the interface between $(Cu, Ni)_6Sn_5$ and Ni–P deposits layer after aging, but fracture at this interface was not the dominant site for immersion Au/Ni–P/Cu and electroless Ni–P/Cu pad.

(Received February 25, 2002; Accepted June 13, 2002)

Keywords: *ball shear test, reliability, isothermal aging, fracture surface, phosphorous-rich nickel layer*

1. Introduction

Compared to more conventional packages, such as the dual-in line package or the quad-flat-pack package, the ball-grid array (BGA) package has the advantages of having higher input/output terminal density, smaller footprint, and higher reliability.[1–3] The BGA package has been successfully applied in many electronic products.[4–6] There are an increasing number of higher density BGA substrates that use immersion Au/electroless Ni for the surface finish. The principal advantage of electroless plating is the ability to meet the requirements of increasing in the terminal density. However, there is insufficient space to allow bussing for the more common electrolytic Au/Ni plating.[7,8] The contact pads for the solder balls on the BGAs usually have an Au/Ni surface finish. Each layer of metal plated on BGA substrates has its own specific functions. A nickel layer is used as a barrier to prevent copper from diffusing into solder balls, because copper will interact with tin to form a Cu–Sn intermetallic compound. This intermetallic compound will then affect the shear strength of solder balls. Gold is plated on the Ni surface of the ball pads not only to improve the wettability, but also to increase the resistance to corrosion.[9,10]

Alternative solder alloys are needed to meet environmental regulations, requirements for greater mechanical reliability, and higher temperature service environments in automobiles and in avionics systems.[11,12] Especially, the Sn–Ag and Sn–Ag–Cu alloys are regarded as having the most potential as lead free solder systems.[13,14]

During soldering, the solder alloy melts and reacts with the pad to form intermetallic compounds at the interface joints. In addition, it can grow through the solid state reaction below the melting temperature of the solder. While forming a thin intermetallic compound layer, by the reaction between the solder and pad, it is desirable to achieve a good metallurgical bond. At the same time, excessive intermetallic compound growth may have a deleterious effect.[15,16]

However, the metallurgical behavior and reliability of BGA joints with Sn–Ag–Cu solder have not been sufficiently studied yet. Therefore, the present work was carried out to investigate the effect of isothermal aging on the reliability of BGA joints with Sn–3.5Ag–0.75Cu solder. Ball shear tests were conducted as a function of the time and temperature for isothermal aging. The interfacial reactions between Sn–3.5Ag–0.75Cu solder and BGA pads with three different surface finishes were also studied.

2. Experimental Procedures

Solder balls used in this study were Sn–3.5Ag–0.75Cu solder with a diameter of 760 μm. The BGA substrates used in this study were commercially available, and thermally enhanced BGA substrates with 421 pads, with each pad having a diameter of 640 μm. The BGA pads with three different surface finishes in this study were, namely, bare Cu pad, electroless Ni–P/Cu pad with Ni–P layer thickness of 7–8 μm, and immersion Au/electroless Ni–P/Cu pad with Ni–P and Au layers of 0.15 and 7–8 μm thickness. The electroless Ni plating deposits a mixture of Ni and phosphorous, because of the use of hypophosphite in the chemical reaction for reducing Ni ions. Electroless Ni layers which contain 15 at%P have an amorphous structure. The temperature of the Ni bath is 88°C and the pH 4.3–4.8. The Au layer is deposited on the Ni–P using an immersion Au bath to prevent the oxidation of Ni. The temperature of the Au bath is 89°C and the pH 5.6–6.2. The solder balls were dipped into flux and then planted on the pads manually and the balls were reflowed by using an IR reflow oven (Japan Pulse Labolataries, INC., RF-430-M2). The peak reflow temperature, the highest temperature of a package, was 250°C and the reflow time at which solder balls melt was 120 s. BGA solder joints were then aged isothermally in a convection oven at 70, 120, 150, and 170°C for various times up to about 100 days. SEM (scanning electron microscopy) was used to study the microstructural morphology of solder

*Corresponding author: sbjung@yurim.skku.ac.kr

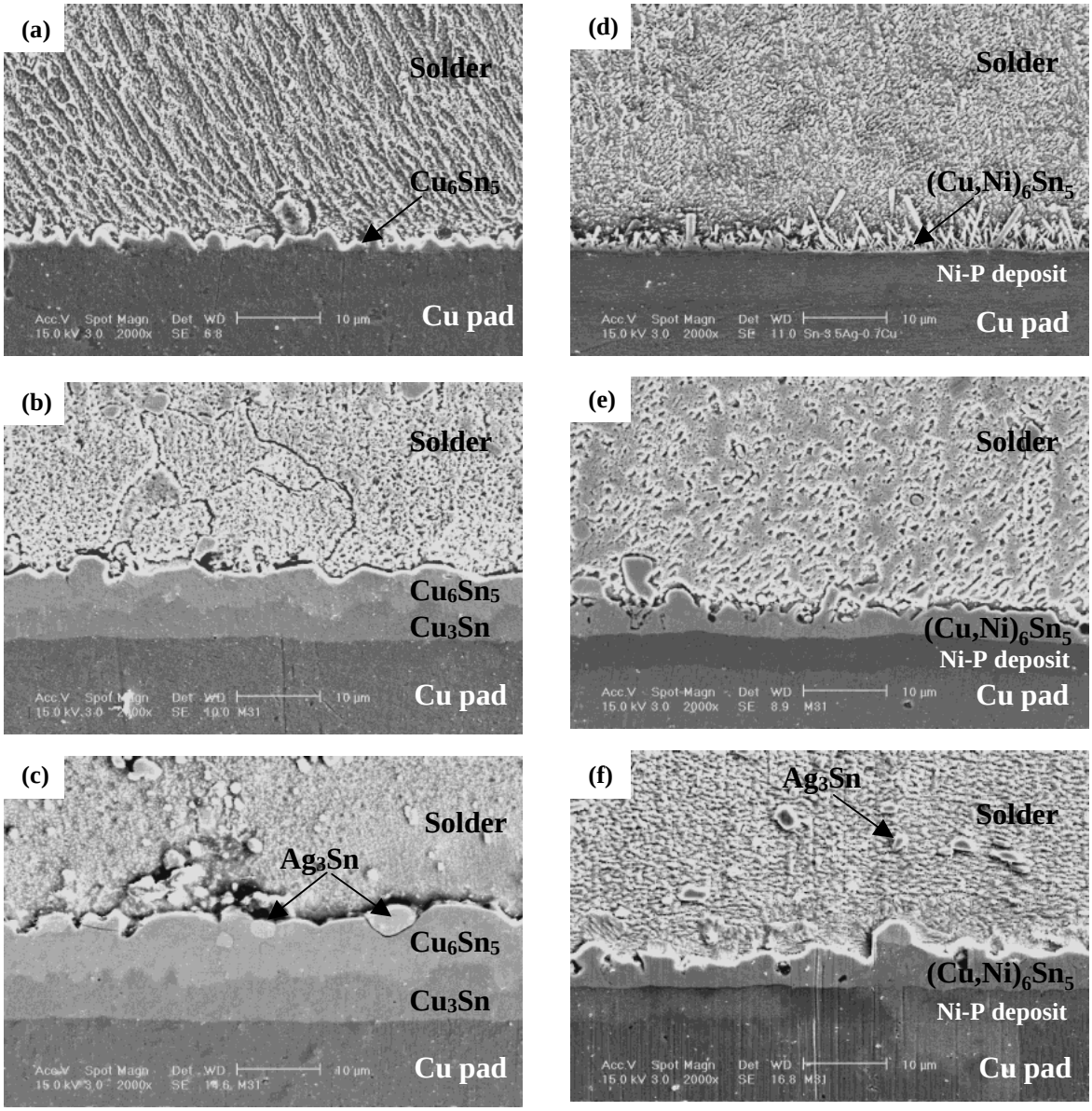

Fig. 1 SEM micrographs of the interface between Sn–3.5Ag–0.75Cu solder and Cu pad (a)–(c), Sn–3.5Ag–0.75Cu solder and immersion Au/Ni–P/Cu pad (d)-(f): as-soldered (a), (d) and after aging at 150°C for 30 days (b), (e) and 100 days (c), (f).

joints before and after isothermal aging. The composition of each phase was determined using the EDX (energy-dispersive X-ray) analysis. Ball shear test as a function of time, temperature and various types of surface finishes was performed. The ball shear strength of resulting BGA joints were measured through the shear tester (Rhesca Co. Ltd., PTR-1000). The failure mode was recorded as either being through the bulk solder or at the intermetallic between the ball and the BGA pads. The blade height was set at 10 μm distant from the substrate and the shearing speed was maintained of 100 μm/s.

3. Results and Discussion

The SEM micrographs of Figs. 1(a)–(c) show the growth of intermetallic layers at the interface between Sn–3.5Ag–0.75Cu solder and Cu pad. In the as-soldered sample, the Cu_6Sn_5 intermetallic compound located at the solder/Cu pad interface was identified by means of EDX analysis, but Cu_3Sn intermetallic was not found as shown in Fig. 1(a). On the other hand, after isothermal aging, the solder/Cu pad interface exhibited a duplex structure of Cu_6Sn_5 and Cu_3Sn intermetallic (see Figs. 1(b) and (c)).

Figures 1(d)–(f) display a series of SEM micrographs showing the growth of intermetallic layers at the interface between Sn–3.5Ag–0.75Cu solder and immersion Au/Ni–P/Cu pads. During soldering, all Au layer on the pad is dissolved into the bulk solder, and the Ni–P layer comes in contact with the molten solder. The Ni atoms diffused inward into the solder, forming only a Ni–Sn intermetallics and P is expelled from the Ni–Sn intermetallic layer.[17] In the case of Ni and Sn interaction, the chunky and needle type Ni_3Sn_4 intermetallics formed at the solder/electroless Ni–P interface is known to be the primary intermetallic compound.[18] According to previous work by Zeng *et al.*,[19] the $(Cu, Ni)_6Sn_5$ intermetallic compound was formed in the coupled of electroless Ni–P/Sn–3.8Ag–0.7Cu solder. The $(Cu, Ni)_6Sn_5$ intermetallic compound in this work is formed between the solder and the electroless Ni–P deposits, which satisfy the report of Zeng

et al.[19] The Cu of Sn–3.5Ag–0.75Cu solder can diffuse into the Ni–P deposit during soldering and aging. It is concluded that the formation of $(Cu, Ni)_6Sn_5$ intermetallic may be due to segregation of Cu between the solder and Ni–P deposit. The Ni concentration in the $(Cu, Ni)_6Sn_5$ intermetallic is 7–9 at%, which is expected because Ni and Cu have solid solution in the Cu–Ni binary phase diagram.[20] Figure 1 also reveals that both the Cu_6Sn_5 and $(Cu, Ni)_6Sn_5$ intermetallic layers thicken, from about 1 μm of Cu_6Sn_5 and 0.5 μm of $(Cu, Ni)_6Sn_5$ in as-soldered joints to about 12.4 μm of Cu–Sn (Cu_6Sn_5+Cu_3Sn) and 4.7 μm of $(Cu, Ni)_6Sn_5$ in joints aged at 150°C for 100 days. After significant aging, the interface between the intermetallic compound and bulk solder becomes smoother. This observation is significant, since it is known that a smooth intermetallics/solder interface, as opposed to a rough surface, degrades the mechanical properties of the joint due to the decreased resistance to shear along the interface. Except for the as-soldered joint, Ag_3Sn intermetallics are present in the bulk solder and in the intermetallic layer.

Figure 2 shows the variation of shear strength with the time and temperature, and various types of BGA pad surface finishes (bare Cu, electroless Ni–P/Cu and immersion Au/Ni–P/Cu pads). The shear strength decreased with the increasing temperature and time irrespective of the deposited layer. A significant decrease in shear strength was noticed for each type of BGA pad after 15 days of isothermal aging. It can be seen from the test results that the shear strengths decrease by 25.3, 23.7 and 20.4% after 100 days of aging at 150°C compared to the strengths measured after as-soldered for Cu pad, electroless Ni–P/Cu pad and immersion Au/Ni–P/Cu pads. It was noticed that the shear strength for both the immersion Au/Ni–P/Cu and electroless Ni–P/Cu pads was consistently higher than that of the Cu pads for all aging conditions. After as-soldered, the shear strengths were measured as 150.5, 182.2 and 179.8 mN for Cu pad, electroless Ni–P/Cu pad and immersion Au/Ni–P/Cu pad, respectively. After aging at 150°C for 100 days, the shear strength changed to 112.4, 139.1 and 143.2 mN for the above pads. Similar to the isothermal aging conditions, the ball shear strengths of immersion Au/Ni–P/Cu pads and electroless Ni–P/Cu pads were very close. Ball shear strength values of the Cu pads were relatively lower than those of the immersion Au/Ni–P/Cu pads and electroless Ni–P/Cu pads. As tests went on, the shear strength of the solder ball decreased approximately parabolic with the duration of the test for all three types of BGA pads. After isothermal aging, the fracture surface showed various characteristics depending on aging temperature, aging time and the types of BGA pad.

Figure 3 shows the fracture surface of BGA Cu, electroless Ni–P/Cu and immersion Au/Ni–P/Cu pad with Sn–3.5Ag–0.75Cu solder before and after aging at 150°C for 100 days. For Cu BGA pad, the ball shear initially occurred through the solder ball but changed to brittle fracture at the interface between the solder ball and the intermetallic region, within the Cu_6Sn_5 intermetallic layer and between the Cu_6Sn_5 and Cu_3Sn intermetallic after isothermal aging at 150°C for 100 days. For immersion Au/Ni–P/Cu and electroless Ni–P/Cu BGA pad, all failures were observed at the solder bulk side and not at the interface, and showed more ductile fracture mode than those of Cu pads. The shear strength of BGA

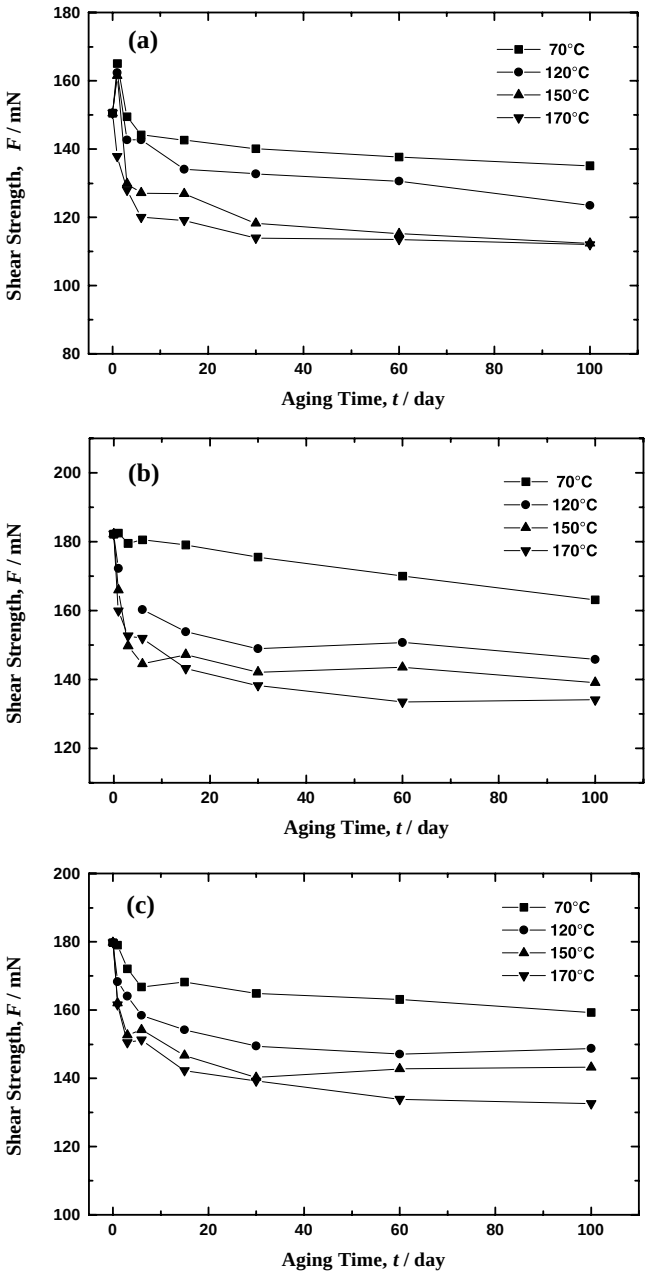

Fig. 2 Variations of the ball shear strength with aging time and temperature: (a) Cu pad, (b) electroless Ni–P/Cu pad and (c) immersion Au/Ni–P/Cu pad.

Cu pad is lower than that on either the immersion Au/Ni–P/Cu or electroless Ni–P/Cu pad, as evidenced by the results in Fig. 2. In the ball shear test, fracture occurs at either interface or in the region with the lowest shear strength. On the Cu pad, after isothermal aging, where two continuous intermetallic compound layers (Cu_6Sn_5 and Cu_3Sn) form, the fracture tends to occur at their interface. It is found that the shear strength between the Cu_6Sn_5 and Cu_3Sn is lower than that between the solder and Cu_6Sn_5 intermetallic. But when the immersion Au/Ni–P/Cu and electroless Ni–P/Cu pads does not form two continuous intermetallic compound layers, the shear strength decreases due to the coarsening of microstructure. This explains why the shear strength between solder and $(Cu, Ni)_6Sn_5$ is higher than that between the Cu_6Sn_5 and solder as well as the Cu_6Sn_5 and Cu_3Sn intermetallic.

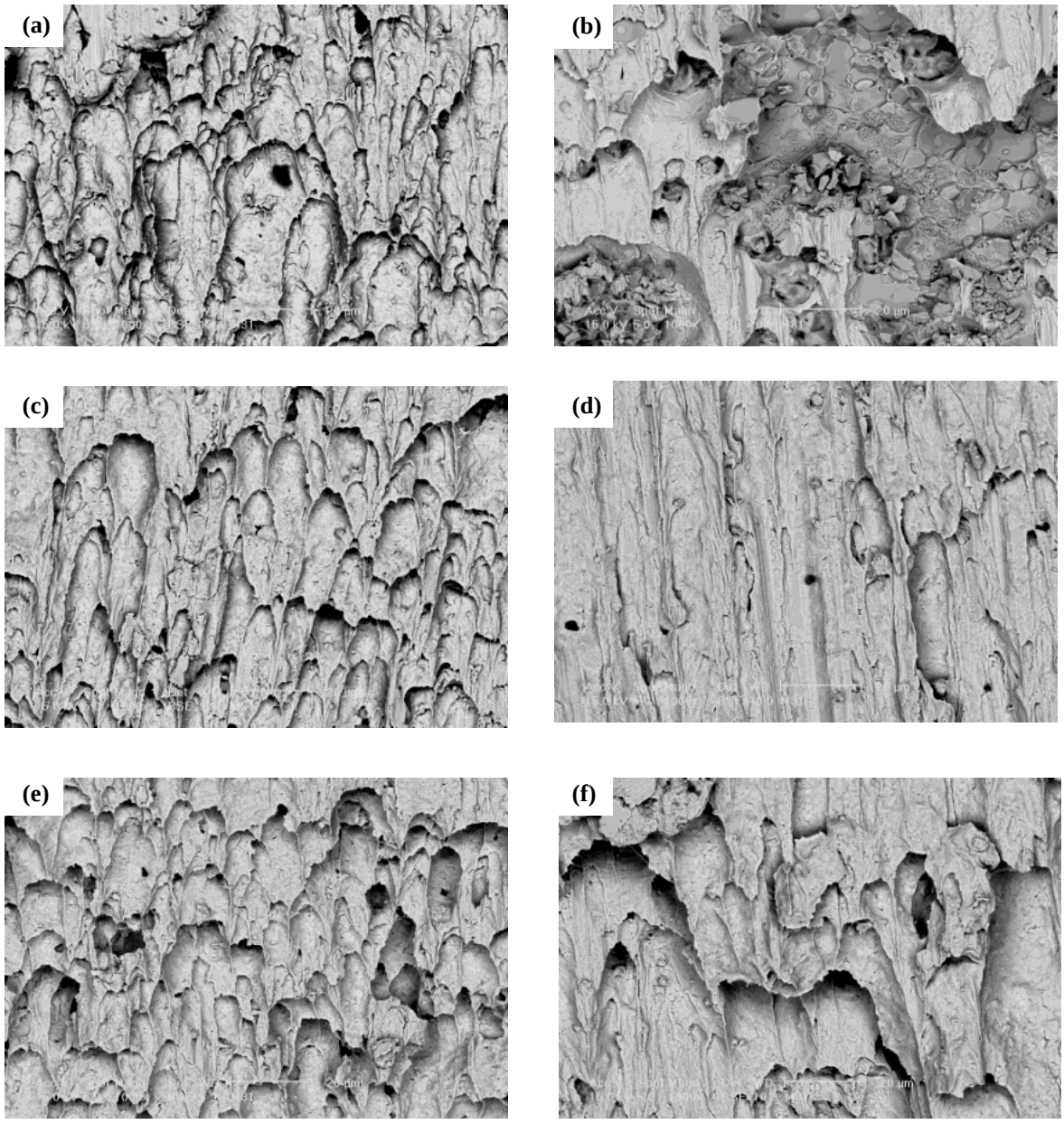

Fig. 3 Fracture surface after ball shear test for solder/Cu pad joint (a), (b), solder/electroless Ni–P/Cu pad joint (c), (d), and immersion Au/Ni–P/Cu joint (e), (f): as-soldered (a), (c), and (e) and after aging at 150°C for 100 days (b), (d), and (f).

Figure 4 shows the fracture surface for Cu BGA pad joints with its EDX analysis after aging at 150°C for 100 days. The fracture occurs at the interface between the solder and Cu_6Sn_5 intermetallic as well as the Cu_6Sn_5 and Cu_3Sn intermetallic. In the EDX analysis, the Cu_6Sn_5 and Cu_3Sn were detected. The fracture plane largely follows the Cu_6Sn_5/Cu_3Sn interface, though cleaved Cu_6Sn_5 particles and intergranular separations in the Cu_6Sn_5 intermetallic layer also appear in the fracture surface. This result suggests relatively weak bonding at the Cu_6Sn_5/Cu_3Sn interface, a conclusion that is supported by the different crystal structure of the two intermetallics.

Also, a thick intermetallic compound layer results in mechanical failure due to volume shrinkage during the transformation from solid phase (Sn and Cu) to the intermetallic compounds.[5] Thick intermetallic compound layer poses potential reliability issues due to an 8.5% and 5% volume shrinkage during the transformation from solid phase to the Cu_3Sn and Cu_6Sn_5 intermetallics.

As shown in Fig. 1, with 100 days of aging at 150°C, the Cu–Sn($Cu_6Sn_5 + Cu_3Sn$) intermetallic thickness increases by 12.4 μm, but the $(Cu, Ni)_6Sn_5$ intermetallic thickness only by 4.7 μm. The thickness of the Cu–Sn($Cu_6Sn_5 + Cu_3Sn$) intermetallic increases faster than that of the $(Cu, Ni)_6Sn_5$ intermetallic. This would create a large internal strain, so the fracture occurs either at the interface between the Cu_6Sn_5 and Cu_3Sn intermetallics or within the Cu_6Sn_5 intermetallic.

Figure 5 shows the SEM micrographs of the interface between solder and immersion Au/Ni–P/Cu pad after aging at 150°C for 100 days. The back-scattered electron imaging of SEM was used to provide more distinguishable boundaries of the interfacial intermetallic layer. In the results of EDX analysis, two other layers were observed between the solder and Ni–P deposit. A P-rich Ni layer was found immediately adjacent to Ni–P deposits. The $(Cu, Ni)_6Sn_5$ intermetallic was

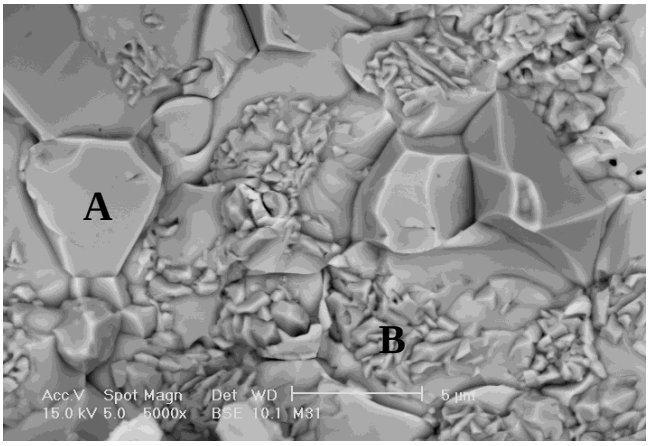

Analysis	Composition (at %)	
	Cu	Sn
A	54.69	45.31
B	74.34	25.66

Fig. 4 Fracture surface of Sn–3.5Ag–0.75Cu/Cu pad joint after aging at 150°C for 100 days, and EDX analyses of points shown in micrograph. Phase identification: A = Cu_6Sn_5, B = Cu_3Sn.

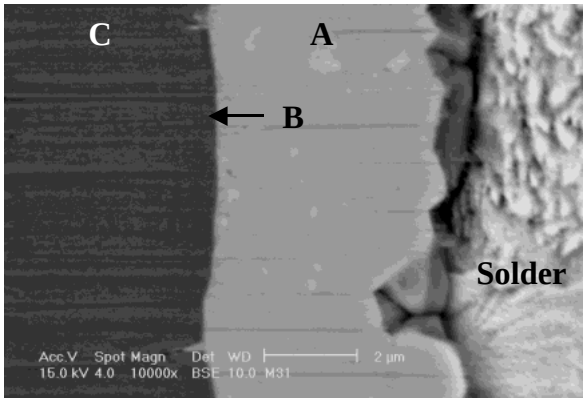

Analysis	Composition (at %)			
	Cu	Ni	Sn	P
A	46.00	8.37	45.63	-
B	-	73.24	-	26.76
C	-	85.17	-	14.83

Fig. 5 Backscattered electron micrograph of the interface between Sn–3.5Ag–0.75Cu solder and immersion Au/Ni–P/Cu pad after aging at 150°C for 100 days, and EDX analyses of points shown in micrograph. Phase identification: A = $(Cu, Ni)_6Sn_5$, B = P-rich Ni layer and C = Ni–15 at%P.

detected between the P-rich Ni layer and solder. The growth of $(Cu, Ni)_6Sn_5$ intermetallic results in a P-rich Ni layer underneath the $(Cu, Ni)_6Sn_5$ intermetallic. The electroless Ni–P deposits used in this study contains about 15 at%P, and the P content in the P-rich Ni layer increases to about 25 at% after 100 days of aging at 150°C. This P-rich Ni layer has been accused of causing the brittle fracture of solder joints,[21] but it this study does not support that a P-rich Ni layer causes brittle fracture. As shown in Fig. 3, the fracture at the P-rich Ni layer was not the dominant failure site for immersion Au/Ni–P/Cu and electroless Ni–P/Cu pads.

During aging, it was expected that Au atoms were diffused back to the interface between solder and intermetallic compound and resulted in the decreasing of bonding strength. Ductility loss of Sn base solder due to the presence of gold is often called gold embrittlement and cited as a reason for failure of solder joints.[22] Also, Mei *et al.*[23] reported that Au–Sn intermetallics caused embrittlement in BGA joints. However, Au was not found remaining at the interface of the BGA pad and solder ball due to the limited spatial resolution of the SEM. A possible explanation is that Au–Sn intermetallics were too rare to detect, since the Au plating is so thin for immersion Au/Ni–P/Cu BGA pads. As shown in Figs. 3(e) and (f), on the immersion Au/Ni–P/Cu pads, all failures are observed as only the ductile fracture inside the solder ball. Also, Syed[24] reported that the ball shear strength favors Sn–Ag–Cu solder over Sn–Pb solder.

From the results above, it is concluded that using Sn–3.5Ag–0.75Cu solder can possibly eliminate the Au embrittlement issue.

4. Conclusion

During isothermal aging, the fracture surface and the ball shear strength of Sn–3.5Ag–0.75Cu solder balls on BGA pads with three different surface finishes were investigated. The following conclusions were obtained:

(1) Irrespective of the deposited layer, the shear strength decreased with increasing temperature and time. Especially, the Cu–Sn(Cu_6Sn_5 + Cu_3Sn) intermetallic was the main contributor of solder joint failure due to a thicker Cu–Sn(Cu_6Sn_5+Cu_3Sn) intermetallic compound layer with larger volume shrinkage after isothermal aging.

(2) The Ni–P deposits layer serve as a diffusion barrier, limiting the Cu from diffusing into the solder and forming the brittle Cu–Sn intermetallics. Also, the fracture at P-rich Ni layer was not the dominant failure site for immersion Au/Ni–P/Cu and electroless Ni–P/Cu pads.

(3) During the aging, on the Cu pad, the failure mode gradually changes from ductile fracture in solder to brittle fracture (i) at the interface between solder and intermetallic compound, (ii) within the intermetallic compound and (iii) between two intermetallic compound layers. However, the failure mode of a solder ball with electroless Ni–P/Cu and immersion Au/Ni–P/Cu pads is different from a Cu pad. After long aging times, all failures were observed as only ductile fracture inside the solder ball. This indicates that using Sn–3.5Ag–0.75Cu solder can possibly eliminate the Au embrittlement issue.

(4) The structure of solder/immersion Au/Ni–P/Cu BGA pad interface after aging at 150°C for 100 days, from solder to the BGA pads, consists of a bulk solder, $(Cu, Ni)_6Sn_5$ inter-

metallic layer, P-rich Ni layer, an amorphous Ni–P deposits with 15 at% phosphorous, and Cu pad. On the other hand, the solder/Cu pad interface exhibits a duplex structure of Cu_6Sn_5 and Cu_3Sn intermetallic.

Acknowledgements

This work was supported by grant No. (R01-2000-00227) from the Basic Research of the Korea Science & Engineering Foundation.

REFERENCES

1) E. Bradley and K. Banerji: IEEE Trans. Comp. Pkg. & Mfg. Technol. **B19** (1996) 320–331.
2) T. A. Nguty, N. N. Ekere, J. D. Philpott and G. D. Jones: Soldering and Surf. Mount Technol. **12** (2000) 35–38.
3) I. Shohji, F. Mori and K. F. Kobayashi: Mater. Trans. **42** (2001) 790–793.
4) S.-W. Ricky Lee and J. H. Lau: Soldering and Surface Mount Technol. **10** (1998) 26–31.
5) P. L. Tu, Y. C. Chan, C. W. Tang and J. K. Lai: Proc. of Electronic Components and Technology Conference, (IEEE, 2000) pp. 1369–1375.
6) C. E. Ho, Y. M. Chen and C. R. Kao: J. Electronic Materials **28** (11) (1999) 1231–1237.
7) R. J. Coyle, A. Holliday, P. Mescher, P. P. Solan, S. A. Gahr, H. A. Cyker, J. K. Dorey and T. I. Ejim: Proc. IEEE/CPMT Int'l Electronics Manufacturing Technology Symposium, (1999) pp. 23–35.
8) F. D. Bruce Houghton: Circuit World **26** (2000) 10–16.
9) S. C. Hung, P. J. Zheng, S. C. Lee and J. J. Lee: Proc. of the 1999 IEEE/CPMT Int'l Electronic Manufacturing Technology Symposium, (1999) pp. 7–15.
10) C. B. Lee, S. B. Jung, Y. E. Shin and C. C. Shur: Mater. Trans. **42** (2001) 751–755.
11) J. A. Kern, M. W. Weiser, C. A. Drewien, F. J. Yost and S. Sackinger: Sandia Report, SAND 96-1431, Sandia Nat. Lab., June (1996) pp. 1–5.
12) S. Jin: JOM 45 (1993) 13.
13) D. R. Flanders, E. G. Jacobs and R. F. Pinizzotto: J. Electronic Materials **26** (1997) 883–887.
14) K. Suganuma and Y. Nakamura: J. Japan Inst. Metals **59** (1995) 1299–1305.
15) G. Ghosh: Acta Mater. **48** (2000) 3719–3738.
16) S. Choi, T. R. Bieler, J. P. Lucas and K. N. Subramanian: J. Electronic Materials **28** (1999) 1209–1215.
17) J. W. Jang, P. G. Kim, K. N. Tu, D. R. Frear and P. Thompson: J. Appl. Phys. **85** (1999) 8456–8463.
18) K. N. Tu and K. Zeng: Mater. Sci. Eng. **R34** (2001) 1–58.
19) K. Zeng, V. Vuorinen and J. K. Kivilahti: Proc. of the 2001 Electronic Components and Technology Conference, (IEEE, 2001) pp. 693–698.
20) T. B. Massalski: *Binary Alloy Phase Diagrams*, Vol. 2, (ASM, Ohio, USA, 1986) pp. 1442–1444.
21) C. Y. Lee and K. L. Lin: Thin Solid Films **229** (1993) 63–75.
22) J. H. Lau: *Ball Grid Array Technology*, (McGraw Hill, Inc., New York, 1995) pp. 400–410.
23) Z. Mei, M. Kaufmann, A. Eslambolchi and P. Johnson: Proc. of the 1998 Electronic Components and Technology Conference, (IEEE,1998) pp. 952–961.
24) A. Syed: Proc. International Symposium on Advanced Packaging Materials, (2001) pp. 143–147.